Epileptic and developmental disorders of the speech cortex: ligand/receptor interaction of wild-type and mutant SRPX2 with the plasminogen activator receptor uPAR

Barbara Royer-Zemmour[1], Magali Ponsole-Lenfant[1], Hyam Gara[1], Patrice Roll[1], Christian Lévêque[2,3], Annick Massacrier[1], Géraldine Ferracci[3], Jennifer Cillario[1], Andrée Robaglia-Schlupp[1], Renaud Vincentelli[4], Pierre Cau[1] and Pierre Szepetowski[1,*]

[1]INSERM UMR910, Université de la Méditerranée, 13385 Marseille, France, [2]INSERM UMR641, Université de la Méditerranée, 13916 Marseille, France, [3]Centre d'Analyse Protéomique de Marseille, IFR11, 13916 Marseille, France and [4]CNRS UMR6098, Université de la Méditerranée, 13288 Marseille, France

Mutations in *SRPX2* (Sushi-Repeat Protein, X-linked 2) cause rolandic epilepsy with speech impairment (RESDX syndrome) or with altered development of the speech cortex (bilateral perisylvian polymicrogyria). The physiological roles of *SRPX2* remain unknown to date. One way to infer the function of *SRPX2* relies on the identification of the as yet unknown SRPX2 protein partners. Using a combination of interactome approaches including yeast two-hybrid screening, co-immunoprecipitation experiments, cell surface binding and surface plasmon resonance (SPR), we show that SRPX2 is a ligand for uPAR, the urokinase-type plasminogen activator (uPA) receptor. Previous studies have shown that uPAR$^{-/-}$ knock-out mice exhibited enhanced susceptibility to epileptic seizures and had brain cortical anomalies consistent with altered neuronal migration and maturation, all features that are reminiscent to the phenotypes caused by *SRPX2* mutations. SPR analysis indicated that the p.Y72S mutation associated with rolandic epilepsy and perisylvian polymicrogyria, led to a 5.8-fold gain-of-affinity of SRPX2 with uPAR. uPAR is a crucial component of the extracellular plasminogen proteolysis system; two more SRPX2 partners identified here, the cysteine protease cathepsin B (CTSB) and the metalloproteinase ADAMTS4, are also components of the extracellular proteolysis machinery and CTSB is a well-known activator of uPA. The identification of functionally related SRPX2 partners provides the first and exciting insights into the possible role of SRPX2 in the brain, and suggests that a network of SRPX2-interacting proteins classically involved in the proteolytic remodeling of the extracellular matrix and including uPAR participates in the functioning, in the development and in disorders of the speech cortex.

INTRODUCTION

How the language areas develop and function represents a crucial scientific issue: language is specific to the human species and remains a mysterious process from several viewpoints. Language has been widely studied through various approaches and in different fields including linguistics, anthropology, archeology, psychology, philosophy, medicine and biology. While considerable progress has been made in the recent years in the analysis of the brain language areas and networks by functional neuroimaging, very little is known on the molecular mechanisms that lead to the appropriate and precise development and functioning of the complex

*To whom correspondence should be addressed at: Inserm UMR910, 'Génétique des Epilepsies Isolées et Associées' (GEIA) Group, Faculté de Médecine de la Timone, 27 Bd J Moulin, 13385 Marseille Cedex 5, France. Tel: +33 33491324386; Fax: +33 33491804319; Email: pierre.szepetowski@univmed.fr

and higher-order anatomical architecture that must be associated with language processing. Convergent evidence at the clinical, electrophysiological and neuroimaging levels has indicated that the perisylvian areas (from Broca's area anteriorly to Wernicke's area posteriorly) play a critical role in the processes associated with expressive and receptive language. Although comparative analyses have led to the identification of a few candidate genes showing differential expression in the perisylvian area during developmental patterning of the cerebral cortex (1,2), this type of approach may not distinguish between the genes that act as key-players and the genes that would only show differential expression as a consequence of other molecular processes. From this viewpoint, the study of human pathologies in which language areas and networks do not develop or function properly represents a promising and quite unique way to start unraveling the mechanisms that are related to language processing. Indeed, the study of one single and large family with autosomal dominant inheritance of oral and speech dyspraxia (MIM 602081) led to the identification of the first 'speech' gene, namely *FOXP2*, that encodes a transcription factor of the forkhead domain family (3). Since then, studies on *in vitro* and *in vivo* models have been done that aim to decipher the cellular and molecular mechanisms that may sustain speech processing and evolution through FOXP2-mediated regulation of transcription (4–6).

SRPX2 (Sushi-Repeat Protein, X-linked 2) is another gene that can be directly associated with altered speech production and abnormalities in brain speech areas. Indeed, mutations in *SRPX2* cause epileptic, speech and developmental disorders of the language cortex (MIM 300642) (7). The pathogenic p.N327S mutation leads to gain-of-glycosylation of the mutant SRPX2 protein and causes seizures of the rolandic (sylvian) brain area with oral and speech dyspraxia and with mental retardation (MIM 300643). The other disease-causing mutation (p.Y72S) occurs in a functional domain of SRPX2 and was identified in one affected male with rolandic seizures and bilateral perisylvian polymicrogyria and in his female relatives with no or mild mental retardation only (MIM 300388). As *SRPX2* mutations cause defects of the rolandic and perisylvian regions, this gene actually represents a promising key to start understanding the functioning and the development of the speech areas in both physiological and pathological conditions. SRPX2 (Genbank NP_055282) is a secreted protein of 465 aminoacids that contains three consensus sushi repeat motifs of approximately 60 aminoacids each. Sushi domains exist in a large variety of organisms from viruses to mammals. They are frequently found in proteins of the complement system—sushi domains are also known as CCP (complement control protein) modules—and in various others including members of the selectin family (8). In the brain, sushi domains may be the basis for the distinct subcellular localizations and physiological actions on synaptic plasticity of the two $GABA_{B1}$ subunit isoforms (9,10). The seizure-related murine protein Sez-6 contains sushi domains and participates in the excitability of cortical neurons (11). In *Drosophila melanogaster*, the sushi-containing protein hikaru genki is secreted at synaptic clefts and is involved in the development of the central nervous system (12). Together with our own findings on the role of SRPX2 in human brain

pathology (7), all these data indicate that proteins with sushi domains participate in important functions in the brain, probably by mediating protein interactions with a large variety of cell adhesion molecules.

SRPX2 (previously known as SRPUL) had been first described in leukemia cells as a secreted protein with dysregulated expression at the transcriptional level (13). Despite its putative importance in brain functioning and development and its involvement in pathologies of the language cortex, the actual role of SRPX2 remains unknown to date. Sushi domains have been involved in various protein–protein interactions, as shown for instance in the interaction of neurocan with L1 (14), in the C4b-binding protein/streptococcal M protein interaction (15), or in the binding of IL15 on its alpha receptor (16,17). Generally, one powerful way to infer the function of a given protein may rely on the identification of its molecular partners. As an example, the function of the epitempin protein LGI1 that is mutated in temporal lobe epilepsies has long remained unpredictable until its subcellular expression was analyzed (18) and the two first LGI1 partners were proposed (19,20). Such an interactome strategy looks particularly attractive in the case of proteins such as SRPX2 that contain modules highly suspected to drive protein interactions. In the present study, we have investigated potential binding partners for the sushi-containing protein SRPX2. We show that SRPX2 is a novel ligand for the urokinase-type plasminogen activator receptor (uPAR) as well as for other members of the extracellular proteolysis system, and that a disease-associated mutant SRPX2 protein displays increased affinity for uPAR. Altogether, our data bring novel and exciting insights on the physiological and pathological processes associated with the functioning and the development of the brain speech areas.

RESULTS

Selection of putative SRPX2 partners by yeast two-hybrid screening

The yeast two-hybrid screening was performed with human SRPX2 full-length coding sequence as a bait and a human adult brain partial cDNA library as target. This yielded about 40 polypeptides, among which 19 corresponded to proteins with known or predicted subcellular localizations consistent with an actual interaction with the secreted SRPX2 protein, i.e. those proteins are known or are predicted to be extracellular and/or to belong to the plasma membrane and the intracellular membrane compartments. In the case of plasma membrane proteins, the domains of interaction as detected by the yeast two-hybrid screening actually corresponded to the extracellular parts of the corresponding full-length proteins (Table 1).

Validation of putative SRPX2 partners by co-IP experiments

In order to confirm the interactions of SRPX2 with some of its putative partners as identified by two-hybrid screening, co-immunoprecipitation (co-IP) experiments were performed. Six out of the 19 putative SRPX2 partners [ADAMTS4,

Table 1. List of SRPX2-interacting peptides as determined by yeast two-hybrid experiments

Name	PBSc	NDC	cDNA access number	Clone seq. (nt)	Protein access number°	DOI (AA)
SORCS2	A	5	NM_020777	1851–2433	NP_065828	651–843
TXNDC4	A	4	NM_015051	913–1303	NP_055866	236–365
SYS1	B	2	NM_033542	235–736	NP_291020	full-length
ATRNL1	C	2	NM_207303	3389–4059	NP_997186	1002–1224
CTSB	C	2	NM_147782	532–818	NP_680092	95–189
EGFL5	C	2	NM_001080497	726–1565	NP_001073966	243–522
NELL2	C	2	NM_006159	837–1190	NP_006150	248–364
PCDH10	C	2	NM_020815	1054–1179	NP_065866	77–117
PSAP	C	2	NM_002778	1361–1686	NP_002769	420–524
ADAMTS4	D	1	NM_005099	1973–2474	NP_005090	516–682
CTGF	D	1	NM_001901	707–1528	NP_001892	168–349
EGFL4	D	1	NM_001410	3458–3814	NP_001401	550–667
FBN1	D	1	NM_000138	6997–7844	NP_000129	2224–2505
LRP4	D	1	NM_002334	1133–1574	NP_002325	330–476
NRCAM	D	1	NM_005010	2421–3395	NP_005001	651–974
PCSK6	D	1	NM_002570	2807–3273	NP_002561	832–969
uPAR	D	1	NM_002659	776–1207	NP_002650	183–327
TNFRSF25	D	1	NM_148966	262–872	NP_683867	59–262
WIF1	D	1	NM_007191	448–982	NP_009122	102–279

The list was elaborated after selection based upon the known and/or predicted subcellular localizations of the corresponding proteins. Access numbers are given according to Genbank at NCBI (http://www.ncbi.nlm.nih.gov/). A confidence score (PBSc, for Predicted Biological Score) was attributed to each interaction as previously described (59). For a given protein, NDC corresponds to the number of different clones that were identified by the yeast two-hybrid screening. When more than one type of clone was identified (PBSc A−C), the clone sequence (seq.) that is indicated corresponds to the sequence shared in common by the different clones. DOI, domain of interaction; nt, nucleotides; AA, amino acids.

cysteine protease cathepsin B (CTSB), NELL2, PCDH10, uPAR and WIF1] were further selected (i) on the basis of their known function in the brain and/or of their possible relationship with the brain disorders caused by *SRPX2* mutations (Table 2), and (ii) because constructs corresponding to the six full-length selected proteins could be obtained and validated at the time this analysis was set up.

The sequences of all six corresponding full-length open reading frames subcloned into pReceiver-M03 or into pAcGFP-N1 expression vectors were verified in each construct and any DNA mutation reverted by *in vitro* mutagenesis wherever appropriate (Supplementary Material, Table S1) in order to obtain the canonical wild-type proteins of interest. All six fusion proteins that could be produced after transient transfection in the appropriate cell line had a GFP tag at the C-terminus, thus allowing fluorescent and immunological detections. Either of the six constructs was co-transfected with a construct allowing the expression of the SRPX2 protein fused with a myc epitope (pcDNA4-SRPX2). Among the six putative SRPX2 partners, one (NELL2) did not yield detectable co-expression with SRPX2, either in HEK293T cells or in COS-7 cells (data not shown). For the five remaining proteins, co-IP experiments were then performed using myc as precipitating antibody. Neither PCDH10 nor WIF1 yielded detectable western blot signals after precipitation with myc antibody, indicating that those two proteins did not associate with SRPX2, at least in the experimental conditions used here (Supplementary Material, Fig. S1A). In contrast, uPAR, CTSB and ADAMTS4 fusion proteins were efficiently and reproducibly co-immunoprecipitated in the presence of the SRPX2 construct, as western blot analysis revealed that the anti-GFP antibody reacted with bands at the expected sizes (uPAR-GFP: 83 kDa; CTSB-GFP: 64 kDa; ADAMTS4-GFP: 117 kDa) of each corresponding

fusion protein (Fig. 1). As a control, no immunoprecipitation of either protein was obtained in the absence of the SRPX2-myc fusion protein (Fig. 1), and a GFP protein directed toward the secretory pathway through its fusion with a signal peptide at its N-terminus, did not co-immunoprecipitate with SRPX2 (Supplementary Material, Fig. S1B). Together with the yeast two-hybrid experiments, the co-IP data obtained here confirmed that uPAR, CTSB and ADAMTS4 interacted with SRPX2.

Expression analysis of SRPX2 and uPAR in the human and rat brains and SRPX2/uPAR co-IP *in vivo*

Among the three SRPX2 partners as confirmed just above (uPAR, CTSB and ADAMTS4), uPAR represented our first and priority interest. uPAR is a key component of the plasminogen activation system (21) and plays an important role in various processes such as coagulation, immunity, angiogenesis, cell proliferation, adhesion and migration. Interestingly and despite its pleiotropic function, the knock-out of *uPAR* in mice mainly leads to enhanced susceptibility to epileptic seizures and to altered neuronal migration and maturation in the neocortex (22,23), all features that are highly consistent with the phenotypes caused by *SRPX2* mutations in human (7).

Reverse transcription polymerase chain reaction (RT−PCR) experiments were performed to study the spatio-temporal pattern of expression of *SRPX2* and *uPAR* transcripts in human and rat brain tissues. *SRPX2* and *uPAR* transcripts could be detected in all brain samples and at all developmental stages that were analyzed (Fig. 2A). We then performed immunohistochemistry experiments to ask whether the human SRPX2 and uPAR proteins were expressed in the same brain territories, and in the rolandic area particularly.

Table 2. Six putative SRPX2 partners selected for co-immunoprecipitation experiments

Name	OMIM number	Role in normal or pathological brain
UPAR (PLAUR; uPA receptor)	173391	Urokinase plaminogen activator (uPA) receptor. Key component of the cell-surface plasminogen activation system. Involved in neuronal migration and maturation and in epilepsy susceptibility in the mouse (36).
CTSB (cathepsin B)	116810	Cysteine protease with both lysosomal and extracellular localizations. May have neuroprotective function in Alzheimer's disease (50). Associated with the pathogenesis of progressive myoclonic epilepsy type 1 (64), a disorder caused by mutations in the CTSB inhibitor cystatin B (49).
ADAMTS4 (aggrecanase 1)	603876	Disintegrin-like and metalloproteinase with thrombospondin type 1 motif. Cleaves various proteoglycans (65,66), which are key players in the regeneration and plasticity of the central nervous system (52).
PCDH10 (protocadherin 10)	608286	δ2 protocadherin adhesion protein. Protocadherins seem to play a central role in the central nervous system (67). PCDH10 particularly is involved in axonal growth (68).
NELL2	602320	Neuron-specific, thrombospondin-like-1 extracellular protein. Involved in neuron survival and in spatial learning in the mouse (69,70).
WIF1	605186	Secreted protein that inhibits the WNT (wingless-type) developmental control proteins. The canonical WNT signaling pathway is involved in neuronal production and in neuronal precursor proliferation (71).

OMIM, Online Mendelian Inheritance in Man (http://www.ncbi.nlm.nih.gov/).

Samples corresponding to the rolandic and to the lateral temporal areas and taken from two non-epileptic autopsy control individuals were analyzed. In all human samples, uPAR and SRPX2-positive neurons were detected in the same areas (Fig. 2B; Supplementary Material, Fig. S2). Those data demonstrated expression of both SRPX2 and uPAR in the rolandic area. We next examined the temporo-spatial expression patterns of the orthologous Srpx2 and Upar rat proteins in the embryonic brain (E16.5) as well as in the brain at birth (P0) and in adults. These experiments showed co-expression of Srpx2 and Upar proteins at all three stages (Fig. 2C; Supplementary Material, Fig. S2). In particular, these data indicated that the Srpx2 and Upar rat proteins are expressed at the same time at a developmental stage (E16.5) that is crucial for neuronal migration.

We next tested whether the human SRPX2 and uPAR proteins associated in the rolandic area. Protein extracts from this brain region were subjected to immunoprecipitation with anti-SRPX2 antibody. Western blot with anti-uPAR antibody revealed a specific band corresponding to the expected size (55 kDa) of the N-glycosylated uPAR protein (Fig. 2D), confirming that SRPX2 and uPAR directly interact in the

human brain area that is the site of physiological and pathological speech processes.

SRPX2 binding to cell-surface uPAR

Next question consisted in testing the binding of SRPX2 to the cell surface of human cells and in asking whether this binding was, at least partly, dependent on uPAR expression. For this purpose, we used COS-7 cells which normally show low expression of uPAR (24) and have been widely used to study uPAR function. As expected, a weak signal was obtained at the surface of non-transfected (parental) COS-7 cells using anti-uPAR antibody (Fig. 3A). As uPAR is anchored to the plasma membrane *via* a glycosyl-phosphatidyl-inositol (GPI) group, the pAcGFP1-N1/uPARstop construct was designed in order to remove the GFP tag at the C-terminus, thus allowing overexpression of GPI-anchored exogenous uPAR at the cell surface. Indeed, much stronger anti-uPAR signals were obtained after pAcGFP1-N1/uPARstop was transiently transfected in COS-7 cells (COS-7/uPAR cells), thus demonstrating efficient expression of exogenous uPAR at the cell surface (Fig. 3A). Next, we sought to determine if SRPX2 could bind stronger to COS-7/uPAR cells than to parental COS-7 cells. For this purpose, COS-7 cells cultured independently were transiently transfected with the pAPtag-SRPX2 expression vector containing the full-length SRPX2 coding sequence fused with the alkaline phosphatase (AP) coding sequence, in order to produce secreted recombinant protein SRPX2 in the extracellular medium. In parallel, COS-7 cells were transfected with the non-recombinant AP pAPtag expression vector as a control. In both cases, protein extracts from the extracellular media were recovered and tested for the presence (pAPtag-SRPX2-transfected cells) or the absence (pAPtag-transfected cells) of SRPX2, respectively (Fig. 3B). These extracts were then used to test for surface binding of COS-7 (parental) and COS-7/uPAR cultured cells. As expected, no AP activity was detected at the cell surface of the parental COS-7 cells and of the COS-7/uPAR cells when the SRPX2-free medium was applied (Fig. 3C). Weak AP signals were obtained at the surface of parental COS-7 cells when the SRPX2-containing medium was used (Fig. 3C). This was not unexpected given that, as mentioned and shown earlier (Fig. 3A), COS-7 cells display low expression of uPAR (24); in addition, the existence at the surface of parental COS-7 cells of one or several SRPX2 receptors different from uPAR cannot be excluded, as other membrane receptors were detected as putative SRPX2 partners, according to our yeast two-hybrid screening data (Table 1). Consistent with the overexpression of uPAR in COS-7/uPAR cells, pattern of much stronger AP signals was obtained at the surface of COS-7/uPAR cells when the SRPX2-containing medium was applied (Fig. 3C). Because yeast two-hybrid experiments suggested that SRPX2 and the extracellular part of uPAR directly interact, and because *in vivo* and *in vitro* co-IP experiments both confirmed the SRPX2/uPAR association, the binding of SRPX2 to the extracellular portion of uPAR is very likely to sustain the reproducible pattern of SRPX2-dependent AP signals at the surface of uPAR-transfected cells, as compared with uPAR-untransfected cells.
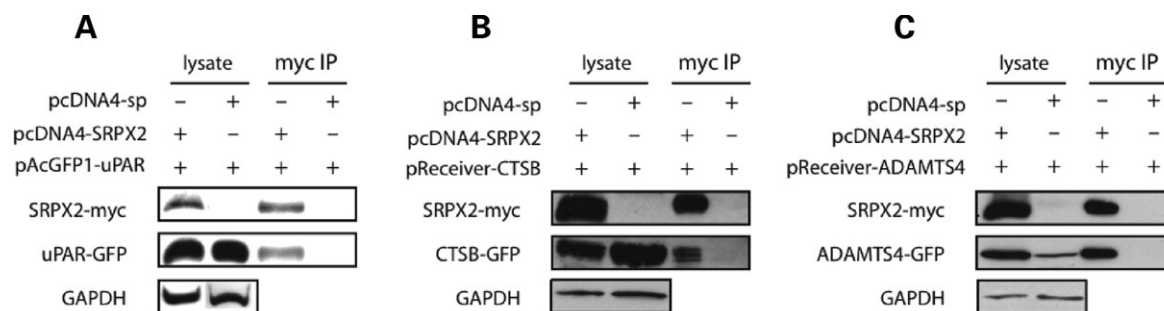
Figure 1. uPAR, CTSB and ADAMTS4 GFP-fusion proteins co-immunoprecipitate with SRPX2-myc in HEK293T cells. Co-IP experiments were performed using anti-myc as precipitating antibody and complexes were resolved by SDS–PAGE, followed by immunoblotting for GFP or myc fusion proteins. (**A**) pcDNA-SRPX2 and pAcGFP1-uPAR constructs were co-transfected in HEK293T cells and the corresponding proteins efficiently produced (lysate). Proteins precipitated with anti-myc antibody (myc IP) were analyzed by immunoblotting. The anti-GFP antibody detected GFP-tagged uPAR protein at the expected size of 83 kDa. The anti-myc antibody detected myc-tagged SRPX2 protein at the expected size of 58 kDa. No band was obtained when the control vector pcDNA4-sp producing the myc tag with only the signal peptide (sp) of SRPX2 at its N-terminus was co-transfected with pAcGFP-uPAR. (**B**) pcDNA-SRPX2 and pReceiver-CTSB constructs were co-transfected in HEK293T cells and the corresponding proteins efficiently produced (lysate). Proteins precipitated with anti-myc antibody (myc IP) were analyzed by immunoblotting. The anti-GFP antibody detected GFP-tagged CTSB protein at the expected size of 64 kDa. The anti-myc antibody detected myc-tagged SRPX2 protein at the expected size of 58 kDa. No band was obtained when pcDNA4-sp was co-transfected with pReceiver-CTSB (**C**). pcDNA-SRPX2 and pReceiver-ADAMTS4 constructs were co-transfected in HEK293T cells and the corresponding proteins efficiently produced (lysate). Proteins precipitated with anti-myc antibody (myc IP) were analyzed by immunoblotting. The anti-GFP antibody detected GFP-tagged ADAMTS4 protein at the expected size of 117 kDa. The anti-myc antibody detected myc-tagged SRPX2 protein at the expected size of 58 kDa. No band was obtained when pcDNA4-sp was co-transfected with pReceiver-ADAMTS4.

Interaction of SRPX2 with the D1 and D2-D3 extracellular domains of uPAR

uPAR is a GPI-anchored receptor that contains three extracellular homologous domains of approximately 90 amino acids each (D1, D2 and D3, from N- to C-terminus). The three domains are members of the Ly-6/uPAR/α-neurotoxin protein domain family and may sustain binding of different known uPAR ligands, with classical uPA binding to D1 and complement S-protein (vitronectin; VTN) binding to D2-D3 (21). In order to precise the site(s) of interaction of SRPX2 with its receptor, *uPAR* partial coding sequences corresponding to various truncated forms of uPAR (Fig. 4A) were inserted into the pAcGFP-N1 expression vector and each corresponding construct was co-transfected with pcDNA4-SRPX2 in HEK293T cells. Various truncated proteins that contained either the D1 (uPARD1-GFP) or the D2-D3 (uPARΔD1-GFP) domains of uPAR were efficiently and reproducibly co-immunoprecipitated in the presence of the SRPX2 construct, as bands at the expected sizes of each corresponding truncated protein (uPARD1-GFP: 60 kDa; uPARΔD1-GFP: 71 kDa) were revealed by western blot analysis using the anti-GFP antibody (Fig. 4B). As expected, fusion proteins containing the two first domains (uPARD12-GFP: 71 kDa) or the three D1, D2 and D3 domains (full-length uPAR-GFP: 83 kDa, and uPAR-D123-GFP: 80 kDa, this latter lacking the C-terminus part of uPAR), also co-immunoprecipitated with SRPX2 (Fig. 4B). Additional bands of lower molecular weights (53 and 62 kDa) could be detected for some of the truncated proteins (uPARD12-GFP and uPARD123-GFP, respectively) and corresponded to non-N-glycosylated forms, as indicated by the decrease in the size of the bands of higher molecular weights when *N*-glycosidase treatment was applied (data not shown). Overall, the data shown here indicated that SRPX2 can associate both with the D1 and with the D2-D3 extracellular parts of uPAR.

Qualitative and quantitative analysis of the wild-type and mutant SRPX2/uPAR interactions

The two disease-causing mutations found in SRPX2, p.Y72S and p.N327S (7), as well as the unique and human-specific p.R75K evolutive mutation that has appeared in SRPX2 since the human–chimpanzee split ∼6–8 millions years ago (25), may have an effect on the SRPX2/uPAR interaction. Co-IP experiments in co-transfected cells showed that the two disease-causing mutant SRPX2 proteins (p.Y72S and p.N327S) as well as the ancestral chimpanzee SRPX2 protein (Genbank ABN46998) with arginine (R) in place of lysine (K) at position 75 (R_{75}), kept interacting with uPAR (Fig. 5) as well as with the two other SRPX2 partners (CTSB and ADAMTS4) validated here (Supplementary Material, Fig. S3).

Co-IP experiments excluded a complete loss of interaction between the mutant SRPX2 proteins and uPAR. Alternatively, (some of) the SRPX2 mutations might well have led to quantitative rather than qualitative changes in the SRPX2/uPAR interaction. Surface plasmon resonance (SPR) experiments were thus performed in order to quantify the binding of uPAR with the wild-type and with the mutant and chimpanzee SRPX2 proteins. Wild-type SRPX2, mutant SRPX2 bearing the pathogenic p.Y72S mutation and ancestral chimpanzee protein with R_{75} were produced in the yeast *Pichia pastoris* and protein production was verified by western blot and by mass spectrometry (Supplementary Material, Fig. S4). The p.N327S gain-of-glycosylation mutant SRPX2 protein could not be produced in sufficient amount despite several attempts. Recombinant uPAR-GST protein was immobilized on the sensor chip surface and different concentrations of analytes (wild-type, mutant and chimpanzee SRPX2 proteins) were injected over the uPAR sensor chip. As expected, wild-type SRPX2 bound to uPAR, with an apparent affinity (K_D) of 114 nM (Table 3) as determined using the single-cycle
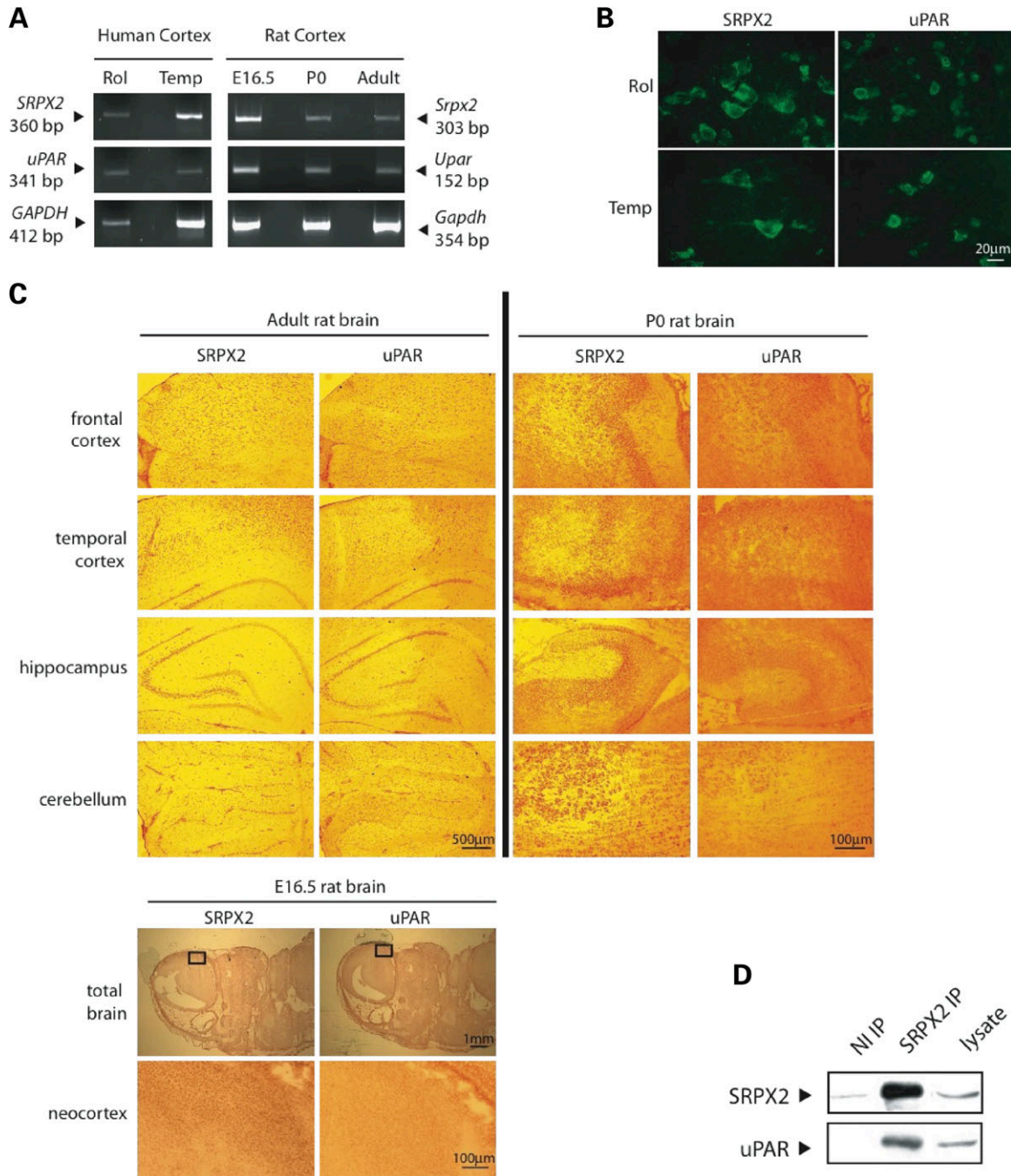
Figure 2. Co-expression and co-IP of SRPX2 and uPAR *in vivo*. (**A**) RT–PCR experiments in human (left) and rat (right) tissues. The sizes of PCR fragments in human and rat are indicated by arrowheads. *GAPDH*: human expression control. *Gapdh*: rat expression control. E16.5: rat brain at embryonic day 16.5. P0: rat brain at birth. Rol: rolandic area. Temp: temporal lobe. (**B**) Immunodetection of SRPX2 and of uPAR in neurons of the human rolandic (Rol) and temporal (Temp) areas. (**C**) Immunodetection of Srpx2 and Upar proteins in the rat brain. (Top) Left: adult rat brain. Right: rat brain at birth (P0). (Bottom) Embryonic rat brain at day 16.5. (**D**) Co-IP of SRPX2 and uPAR in the human rolandic area. Protein extracts from the rolandic area were immunoprecipitated with anti-SRPX2 antibody (SRPX2 IP) or with non-immune (control) rabbit IgG (NI IP). The complexes were resolved by SDS–PAGE, followed by immunoblotting for uPAR or SRPX2.

kinetic method that consists in sequential injection of increasing concentrations (26,27). Consistent with the co-IP data, the p.Y72S mutant SRPX2 protein and the chimpanzee SRPX2 protein also bound to uPAR (Table 3). However, compared with wild-type SRPX2, the p.Y72S SRPX2 pathogenic

mutant displayed a 5.8-fold increase in binding affinity for uPAR ($K_D = 19.6$ nM). Interestingly, the R$_{75}$ SRPX2 chimpanzee protein also had a comparable increase (7.2-fold) in uPAR binding affinity ($K_D = 15.8$ nM), as compared with its human counterpart (wild-type SRPX2). Overall, the pathogenic
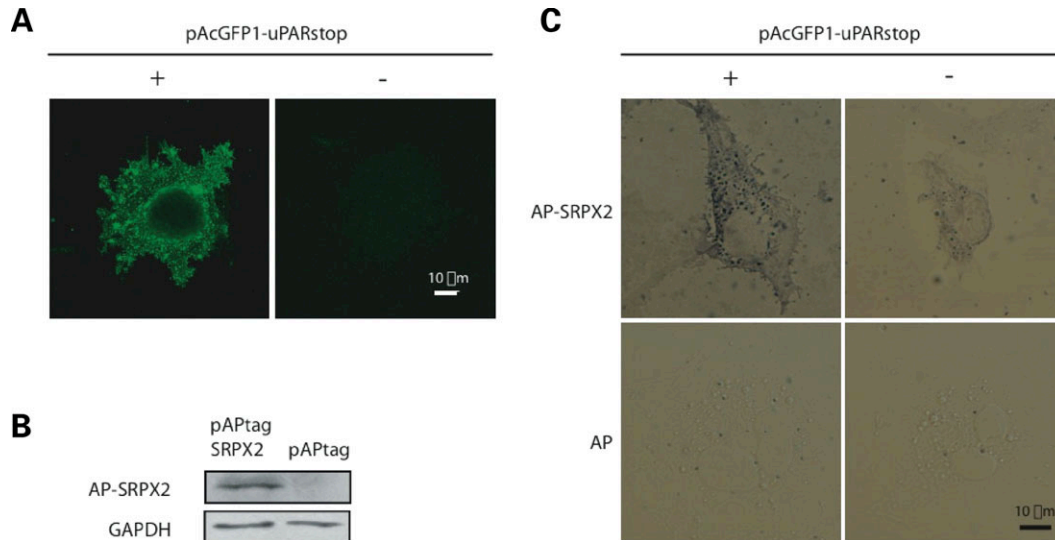
Figure 3. SRPX2 binding to uPAR at the cell surface of transfected COS-7 cells. (**A**) uPAR immunodetection with anti-uPAR antibody at the surface of untransfected (parental) COS-7 cells ($-$) and at the surface of pAcGFP1-uPARstop transfected (COS-7/uPAR) COS-7 cells ($+$). Parental cells show weak expression of uPAR at the cell surface while COS-7/uPAR cells show strong expression of uPAR at the cell surface. (**B**) Production of alkaline phosphatase (AP)-SRPX2 fusion protein in the extracellular medium of COS-7 cells. COS-7 cells were transfected with pAPtag-SRPX2 (left) or with pAPtag (right) vectors. Protein extracts from the extracellular media were resolved by SDS–PAGE, followed by immunoblotting with anti-SRPX2 antibodies. AP-SRPX2 fusion protein was detected only when the pAPtag-SRPX2 was used. No SRPX2 fusion protein was detected when the pAPtag non-recombinant vector was used. The secreted isoform of GAPDH (63) was used as a control of protein extraction. (**C**) SRPX2 binding at the cell surface of uPAR-transfected COS-7 cells (COS-7/uPAR cells). Untransfected (parental) cells ($-$) or cells transfected with pAcGFP1-uPARstop ($+$) were incubated with AP-SRPX2 (top) or with AP (bottom) as a control. No AP activity was detected at the cell surface in the absence of AP-SRPX2. Much stronger AP signals were observed at the cell surface of COS-7/uPAR cells compared with parental COS-7 cells.
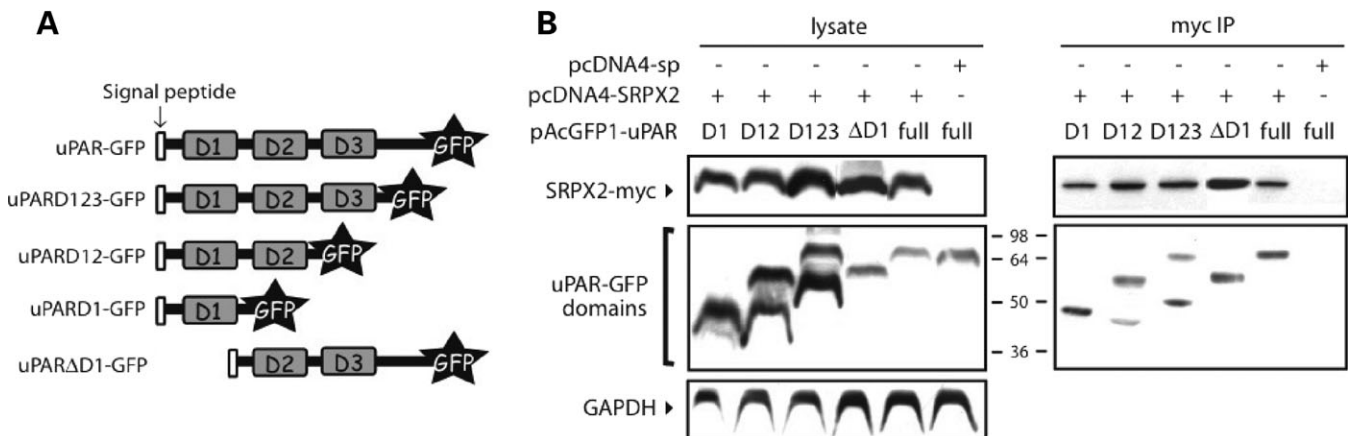
Figure 4. SRPX2 interacts with the D1 and with the D2-D3 domains of uPAR. (**A**) Structural organization of uPAR constructs. (**B**) Truncated uPAR-GFP fusion proteins co-immunoprecipitate with SRPX2-myc in HEK293T cells. pcDNA-SRPX2 and the various pAcGFP1-uPAR constructs were co-transfected in HEK293T cells and the corresponding proteins efficiently produced (lysate). Proteins precipitated with anti-myc antibody (myc IP) were analyzed by immunoblotting for GFP fusion proteins. The anti-GFP antibody detected GFP-tagged truncated (D1, D12, D123, ΔD1) and full-length (full) uPAR proteins. The additional bands of lower molecular weights that could be observed (D12, D123) corresponded to non-N-glycosylated forms of the corresponding truncated protein. The anti-myc antibody detected myc-tagged SRPX2 protein at the expected size (58 kDa). No band was obtained when the control vector pcDNA4-sp producing the myc tag with only the signal peptide (sp) of SRPX2 at its N-terminus was co-transfected with pAcGFP-uPAR.

p.Y72S and the evolutive p.R75K mutations that have occurred in the same hypervariable loop of the first sushi domain of SRPX2 (25) both led to a modification in the *in vitro* affinity for uPAR: the p.R75K evolutive mutation (from R_{75} in non-human primates to K_{75} in human) was associated with a decrease in the SRPX2/uPAR affinity, and the p.Y72S pathogenic mutation was associated with an increase in the SRPX2/uPAR affinity.

DISCUSSION

SRPX2 mutations cause disorders of the language cortex and cognition such as rolandic epilepsy with speech dyspraxia (RESDX syndrome) and rolandic epilepsy with bilateral perisylvian polymicrogyria (7). We show here that the secreted SRPX2 protein is a novel ligand for uPAR, the receptor for the plasminogen activator of the urokinase-type.
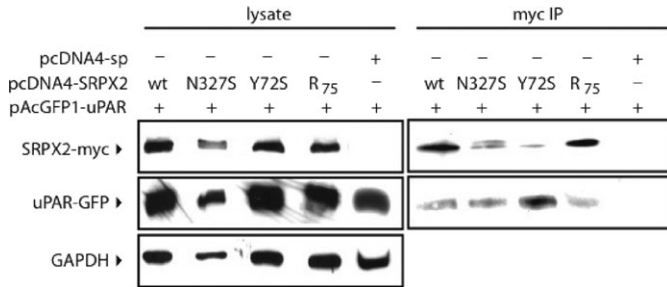
Figure 5. Interaction of mutant SRPX2 proteins with uPAR. Either pcDNA-SRPX2 construct (wt, N327S, Y72S or R$_{75}$) and the pAcGFP1-uPAR construct were co-transfected in HEK293T cells and the corresponding proteins efficiently produced (lysate). Complexes precipitated with anti-myc antibody (myc IP) were resolved by SDS–PAGE, followed by immunoblotting for GFP or myc fusion proteins. The anti-myc antibody detected myc-tagged SRPX2 protein at the expected size of 58 kDa. For all co-IP with wild-type, disease-causing mutant (p.Y72S, p.N327S) and chimpanzee (R$_{75}$) SRPX2 proteins, the anti-GFP antibody detected GFP-tagged uPAR protein at the expected size of 83 kDa. No band was obtained when the control vector pcDNA4-sp producing the myc tag with only the signal peptide (sp) of SRPX2 at its N-terminus was co-transfected with pAcGFP-uPAR.

Table 3. Summary of surface plasmon resonance kinetic data

SRPX2	k_{on} (M^{-1}s^{-1})	k_{off} (s^{-1})	K_D (M)
wt	$7.03 \pm 4.5 \times 10^4$	$8.64 \pm 6.01 \times 10^{-3}$	$114 \pm 31 \times 10^{-9}$
p.Y72S	$6.86 \pm 0.68 \times 10^5$	$1.34 \pm 0.093 \times 10^{-2}$	$19.6 \pm 2.2 \times 10^{-9}$
R$_{75}$	$1.05 \pm 0.36 \times 10^5$	$1.69 \pm 0.94 \times 10^{-3}$	$15.8 \pm 5 \times 10^{-9}$

The SRPX2/uPAR interaction was suggested by yeast two-hybrid analysis and was subsequently confirmed both by *in vitro* and *in vivo* co-IP experiments and by SPR. As measured by three independent SPR experiments, the average strength of the *in vitro* SRPX2/uPAR association was at $K_D = 114$ nM. Hence, several independent methods all concluded in favor of the interaction of SRPX2 with uPAR. uPAR is composed of three homologous domains (D1, D2 and D3) that are members of the Ly-6/uPAR/α-neurotoxin protein domain family. While yeast two-hybrid screening had indicated interaction of SRPX2 with the D2-D3 part of uPAR, co-IP experiments with various truncated forms of uPAR showed that SRPX2 could interact not only with D2-D3 but also with the D1 domain of uPAR. Such a versatile binding to either the D1 or the D2-D3 domains had already been demonstrated in the case of kininogen, a well-known uPAR ligand (28). While other uPAR ligands can classically bind either to D1 in the case of uPA (urokinase plasminogen activator), or to D2-D3 in the case of complement S-protein (VTN) (21), recent structural analyses indicated that all three domains actually participate in the formation of the uPA/uPAR and uPA/VTN/uPAR complexes (29,30).

The ligand/receptor SRPX2/uPAR relationship was also further demonstrated by cell surface binding, using a secreted AP fusion protein of SRPX2 that bound much stronger to the surface of COS-7 cells when transfected with uPAR. A secreted uPAR isoform (suPAR) can also be generated and our data do not exclude the possible binding of SRPX2 to both types (secreted and membrane-anchored) of uPAR proteins, as shown in the case of the uPA/uPAR interaction (31).

The weaker but visible binding of SRPX2 to the cell surface of COS-7 cells in the absence of exogeneous uPAR expression might well be due to the basic expression of native uPAR at the surface of COS-7 cells (24). Alternatively, the existence of other SRPX2 receptors at the cell surface of COS-7 cells is likely, as yeast two-hybrid screening led us to identify several other putative SRPX2 plasma membrane receptors. Generally, the existence of several SRPX2 partners in the central nervous system would be consistent with a pleiotropic role of SRPX2 in the brain, especially if the partners are not all expressed in the same territories, and at the same time during brain development and maturation. As a matter of fact, the two disease-causing *SRPX2* mutations reported to date, led to overlapping and related albeit different brain disorders of the speech areas (7). From this point of view, several putative SRPX2 partners detected by the yeast two-hybrid screening (Table 1) have interesting functions, such as the δ2 protocadherin PCDH10. Neither PCDH10 nor WIF1 co-immunoprecipitated with SRPX2 in the experimental conditions used here; they might obviously represent false-positive interactions with SRPX2. Noteworthingly, mutations in another δ2 protocadherin, PCDH19, also lead to epilepsy with cognitive impairment (32), and the δ2 protocadherin PCDH17 shows enriched expression in cortical circuits involved in higher functions, including language (2). Although the co-IP experiments performed here did not confirm a direct SRPX2/PCDH10 association *in vitro*, an interaction *in vivo* cannot be ruled out. Moreover, interaction of SRPX2 with the phylogenetically related PCDH17 and PCDH19 proteins (33) is not excluded, as some SRPX2 receptors could have escaped detection by the yeast two-hybrid method.

Demonstration of the SRPX2/uPAR ligand/receptor interaction has important consequences for the understanding of SRPX2 and uPAR functions in the human brain. The uPAR system has got well-known function in a broad range of physiological and pathological processes such as fibrinolysis, immune responses, inflammation, angiogenesis, cell growth and cancer metastasis (21,34,35). In addition to this pleiotropic role, mice carrying a targeted mutation of the *Upar* gene have brain cortical alterations consistent with the impairment of GABAergic interneurons migration and maturation (22). GABAergic activity is involved in the susceptibility to epileptic seizures (36) and also participates in the coordinated generation and migration of interneuron and pyramidal populations (37,38). Together with the *Upar* knock-out phenotype, the data presented here strongly suggest that uPAR plays an important role in the human brain as well.

The SRPX2 p.Y72S disease-causing mutation led to 5.8-fold increase in the SRPX2/uPAR affinity *in vitro*. The quantitative modification of the SRPX2/uPAR interaction may well have participated in the epileptic and polymicrogyric phenotypes caused by p.Y72S. Consistently, and as stated earlier, the murine *Upar* knock-out model also presented with increased susceptibility to epileptic seizures and with altered neuronal migration and maturation (22). Moreover, both the SRPX2 and uPAR human proteins showed co-expression in the rolandic area, which is the site of the seizures in the patients. Consistent with the phenotype of abnormal cortical gyration, co-expression of Srpx2 and Upar was also detected at the period of neuronal migration and

maturation in the embryonic rat brain. The p.Y72S mutation lies in the critical loop of the first sushi domain of SRPX2 (25). The hypervariable loop of the sushi domains is classically involved in protein–protein interactions and is the site of pathogenic mutations in other sushi-containing proteins (15,39–41). Hence, it is not surprising that the p.Y72S amino acid change in this loop leads to modified SRPX2/uPAR interaction. The SRPX2/uPAR gain-of-affinity may lead to actual gain-of-function of uPAR or conversely may lead to uPAR loss-of-function, for instance by competing with another uPAR ligand. Sufficient amounts of recombinant SRPX2 protein bearing the other and gain-of-glycosylation disease-causing mutation (p.N327S) (7) could not be produced. Whether p.N327S also leads to increased SRPX2/uPAR affinity thus remains undetermined—although co-IP experiments showing conserved qualitative interaction of mutant p.N327S SRPX2 with uPAR in mammalian cells did not argue against such a hypothesis.

Pronounced species specificity of the binding of various natural and artificial ligands to uPAR had already been reported (42). Changes in the SRPX2/uPAR association might have participated in the patterning of the speech areas during higher primates evolution, as the unique and human-specific evolutive mutation (p.R75K) that distinguishes the human and chimpanzee SRPX2 orthologs (25) and that—like p.Y72S—has occurred in the critical loop of the first sushi domain of SRPX2 also led to decreased (7.2-fold) SRPX2/uPAR affinity. Remarkably, the human pathogenic (p.Y72S) and the chimpanzee (R_{75}) SRPX2 proteins had uPAR apparent affinities in the same range ($K_D = 19.6$ and $K_D = 15.8$ nM, respectively), whereas the apparent affinity of human wild-type SRPX2 with uPAR was one order of magnitude weaker ($K_D = 114$ nM).

Several known uPAR-mediated pathways might be altered by the p.Y72S SRPX2 pathogenic mutation. Altered proteolysis-independent signaling *via* various uPAR plasma membrane co-receptors (35) could be involved. Alternatively, alteration of the SRPX2/uPAR interaction might also directly disturb synaptic functioning through the classical proteolytic role of uPAR in the pericellular conversion of plasminogen into plasmin (43). Interestingly, the plasminogen activators of the urokinase (uPA, the uPAR ligand) and of the tissue (tPA) types have already been associated with cognitive and epileptic phenotypes (44–46). Neuronal migration could also be impaired *via* altered uPAR-dependent cleavage and activation of the precursor of hepatocyte growth factor (HGF) (47). The participation of SRPX2 in the extracellular matrix proteolysis pathway is a particularly attractive possibility as two more SRPX2 partners identified by yeast two-hybrid and co-IP experiments in the present study, CTSB and the metalloproteinase ADAMTS4, can also act as extracellular proteases. Generally, the remodeling of the extracellular matrix plays critical role in the development and in the functioning of the brain and matrix members of the extracellular proteolysis cascades have already been involved in various brain disorders. Examples include the serine protease neurotrypsin in non-syndromic mental retardation (48), the cysteine protease inhibitor cystatin B in the progressive myoclonic epilepsy (EPM1) of the Unverricht-Lundborg type (49) and CTSB itself in Alzheimer's disease (50). CTSB cleaves the

inactive form of uPA, and uPAR in turn is cleaved by uPA and by metalloproteases (34). ADAMTS4 (a disintegrin and metalloproteinase) itself influences neuronal phenotype (51). CTSB and ADAMTS4 can even be part of the same proteolysis pathway as they both can cleave aggrecan, a sushi-containing member of the matrix proteoglycans that in turn have important functions in regeneration and plasticity of the central nervous system (52). Together with uPAR, CTSB and ADAMT4 may thus form a single functional network. CTSB and ADAMTS4 still associated with the mutant and chimpanzee SRPX2 proteins that could be studied here; whether such binding is altered quantitatively by SRPX2 mutations remains to be determined.

While numerous studies point for an important role of the ion channel subunits in the genesis of acquired and inherited human epilepsies (53,54), alterations in the extracellular proteolysis system might represent an important and underestimated human epileptogenic mechanism as well. Similarly, the SRPX2/uPAR-associated pathways might be involved in bilateral perisylvian polymicrogyria, the molecular mechanisms of which are poorly known (55,56). The SRPX2/uPAR interaction identified here thus provides a first key to unravel the function of SRPX2 and of uPAR in the human brain and the complicated and still largely unknown processes that sustain the functioning, the development and disorders of the speech areas such as rolandic epilepsy, speech impairment and perisylvian polymicrogyria—a disorder of brain neuronal migration and maturation leading to abnormal cortical gyration.

Finally, the flexibility of uPAR enables its interaction with a wide variety of ligands (29). While uPAR interactions with several ligands and co-receptors have already been described (34), as also indicated at the Human Protein Reference Database (http://www.hprd.org/), there still is an intensive search for novel uPAR interacting molecules. It is thus of broad interest to note that SRPX2 as a novel uPAR ligand may represent a novel target for the design of new therapeutic molecules that would regulate some of the numerous and crucial uPAR-dependent physiological and pathological processes, such as matrix degradation, cell adhesion and migration, clot lysis, proliferation and angiogenesis, apoptosis, cell growth and metastasis.

MATERIALS AND METHODS

Yeast two-hybrid screening

Yeast two-hybrid screening was performed by Hybrigenics, S.A., Paris, France (http://www.hybrigenics.com). The coding sequence for amino acids 24–464 of SRPX2 (GenBank accession number NP_055282) was PCR-amplified and cloned into pB27 as a C-terminal fusion to LexA (N-LexA-SRPX2-C). The construct was checked by sequencing the entire insert and used as a bait to screen a random-primed human adult brain cDNA library constructed into pP6. pB27 and pP6 derive from the original pBTM116 (57) and pGADGH (58) plasmids, respectively. Ninety-one million clones (9.1-fold the complexity of the library) were screened using a mating approach with Y187 (mat-α) and L40DGal4 (mat-α) yeast strains as previously described

(59). A total of 197 His$^+$ colonies were selected on a medium lacking tryptophan, leucine and histidine. The prey fragments of the positive clones were amplified by PCR and sequenced at their 5′ end and 3′ end junctions. The resulting sequences were used to identify the corresponding interacting proteins in the GenBank database (NCBI) using a fully automated procedure. A confidence score (PBSc, for predicted biological score) was attributed to each interaction as previously described (60).

Reverse transcriptase PCRs

Total RNAs from human autopsy brain samples corresponding to the temporal lobe and to the rolandic area and obtained through the Netherlands Brain Bank from two donors were prepared by Trizol extraction, according to the manufacturer's protocol (Invitrogen). Total RNAs from various areas of the adult rat brain, from rat brain at birth (P0) and from embryonic rat brain at stage E16.5, were prepared by Trizol extraction. RT reactions were performed from total RNAs (1 μg) using oligo(dT) primer and the SuperScript II Rnase H2 Reverse Transcriptase (Invitrogen), according to the manufacturer's instructions. One-twentieth of the reaction product was used for PCR amplification of 30 cycles with specific primers for human *SRPX2*, *uPAR* and *GAPDH* genes and their rat counterparts (Supplementary Material, Table S1) in a 9700 DNA thermocycler (Applera).

Generation of constructs

Human wild-type and p.N327S mutant *SRPX2* corresponding coding sequences were amplified by RT–PCR from fibroblasts total RNAs of one control individual and of one RESDX patient (7), respectively, and subcloned into the appropriate vectors (see later). For co-IP experiments, the pcDNA4-SRPX2 constructs were obtained by RT–PCR amplification (primers TagF and TagR2) of the coding sequences of wild-type and p.N327S SRPX2 proteins and subsequent subcloning into pcDNA4/TO/mycHis (Invitrogen) in order to generate wild-type and mutant SRPX2-myc fusion proteins. The p.Y72S mutation and the chimpanzee variation (R at position 75 of SRPX2: R$_{75}$) were introduced into the wild-type construct using the XL Quickchange mutagenesis kit (Stratagene). For protein production in *P. pastoris*, the coding sequences of wild-type and p.N327S SRPX2 proteins were RT–PCR amplified with primers PICZ-F and PICZ-R2 and subcloned into the pPICZ production vector (Invitrogen). p.Y72S and R$_{75}$ were introduced into the wild-type construct using the XL Quickchange mutagenesis kit (Stratagene). Expression vectors containing the *ADAMTS4*, *CTSB*, *NELL2*, *PCDH10* and *WIF1* full-length coding sequences subcloned into p-Receiver-M03 were obtained commercially (Genecopeia Ltd). Full-length and partial human *uPAR* coding sequences were amplified by RT–PCRs from total RNAs of one control autopsy brain sample, using various combinations of primers: uPAR-F and uPAR-R (pAcGFP1-uPAR), uPAR-F and uPARD1-R (pAcGFP1-uPARD1), uPAR-F and uPARD2-R (pAcGFP1-uPARD12), uPAR-F and uPARD3-R (pAcGFP1-uPARD123), uPARD2-F and uPAR-R2 (pAcGFP1-uPARΔD1). The various *uPAR* constructs were obtained by subcloning into pAcGFP1-N1 (Clontech), in order to produce fusion proteins with GFP tag at the C-termini. Control constructs that contained only the signal peptide of SRPX2 (pcDNA4-sp) and of uPAR (pAcGFP1-sp) were obtained by RT–PCR amplification of the corresponding coding sequences (SRPX2 signal peptide: primers TagF and SRPX2signal-R; uPAR signal peptide: primers uPAR-F and uPARsignal-R) and subcloning into pcDNA4/TO/mychis and into pAcGFP1-N1, respectively. For AP experiments, the cDNA corresponding to a truncated SRPX2 protein lacking its signal peptide was amplified by RT–PCR (primers SRPX2-deltaSP-F and SRPX2-R) and inserted into pAPtag-5 plasmid at the C-terminus of the AP tag (pAPtag-SRPX2). In order to allow for the accurate expression of a uPAR protein able to anchor to the plasma membrane through a GPI group, a stop codon was reintroduced into the pAcGFP1-N1/uPAR construct a the end of the uPAR coding sequence and just 5′ to the GFP coding sequence (pAcGFP1-N1/uPARstop) using the XL Quickchange mutagenesis kit (Stratagene) and the appropriate primers. All insert sequences of the constructs used in this study were confirmed by automated sequencing (GATC Biotech) and any unwanted mutation was reverted with the XL Quickchange mutagenesis kit (Stratagene) and using the appropriate primers. The list of all primers used for the constructs and for mutagenesis is given in Supplementary Material, Table S1.

Cell cultures and transfections

Human embryonic kidney (HEK293T) cells and African green monkey kidney fibroblast (COS-7) cells were grown in 5% CO2 at 37°C in DMEM nutrient mixture (Lonza) supplemented with 2 mM glutamine, 100 U/ml penicillin, 100 μg/ml streptomycin, 0.25 μg/ml amphotericin and 10% fetal calf serum. When cells reached 80–90% confluence, they were harvested with 0.25% trypsin and 0.05% EDTA in 10 mM sodium phosphate, 0.15 M NaCl, pH 7.4 buffer (PBS, phosphate-buffered saline) and aliquots of dissociated cells were plated on 100 mm diameter Petri dishes. At 60% confluence, HEK or COS-7 cells were transiently transfected with the appropriate plasmids using the JetPei (PolyPlus Transfection) kit and according to the manufacturer's protocol.

Surface binding assays of AP fusion proteins

AP-tagged fusion SRPX2 protein was produced by transient transfection of COS-7 cells with pAPtag-5-SRPX2 recombinant plasmid (pAPtag-SRPX2) (61). As a control, AP was produced by transfecting the non-recombinant pAPtag-5 plasmid (pAPtag). After 24 h of culture in DMEM medium, transfected cells were grown for an additional 48 h- period in OptiMEM medium (Gibco). The extracellular media were then recovered and concentrated 8-fold on Amicon columns (Millipore) and checked for the presence of AP-SRPX2 fusion protein by SDS–PAGE and immunoblotting (Fig. 3) using anti-SRPX2 antibody (1/500, PTG-Lab; Supplementary Material, Fig. S5).

Parental (untransfected) COS-7 cells or COS-7 cells that had been transfected with pAcGFP1-N1/uPARstop (COS-7/uPAR) were plated 5 h after transfection in four-well coated slides (Lab-tek II CC2, Nunc). Forty-eight hours later, slides were washed twice with Hank's balanced salt solution

(HBAS) and the cells were incubated with equally concentrated AP or AP-SRPX2 for 90 min at 37°C. Cultures were then washed six times with HBAS. Cells were fixed with 4% paraformaldehyde for 15 s. at room temperature and washed two times in HBS (10 mM Hepes pH7, 150 mM NaCl). Slides were incubated at 65°C for 100 min to heat-inactivate the endogenous AP activity, and the AP-SRPX2 binding was revealed in the presence of nitro blue tetrazolium and BCIP (5-bromo-4-chloro-3-indolyl phosphate) (Vector). Slides were mounted in Aquatex (Merck). Sections were observed with a microscope (Leica, CTR5000) and camera (Leica DFC300FX).

Co-IP experiments

Co-IP experiments using transfected HEK293T cells were done as follows: 48 h after co-transfection with the appropriate constructs, HEK293T cells were lysed in 50 mM Tris, pH 7.4, 1% Triton X-100, 10 mM $MgCl_2$ and a cocktail of protease inhibitors. After centrifugation (15 000g, 4°C, 10 min), the lysate was precleared 2 h on 50 µl of anti-IgG Agarose beads (Sigma). One microgram of rabbit anti-myc antibody (Sigma) was also incubated on 50 µl of anti-IgG Agarose beads for 2 h at 4°C. Precleared lysates were then incubated on antibody-coupled beads overnight at 4°C. Non-specific binding was removed from the agarose beads by washing twice with the lysis buffer, twice with 50 mM Tris, pH 7.4, 150 mM NaCl and twice with 50 mM Tris, pH 7.4. The immunoprecipitated SRPX2 protein and SRPX2 partner were dissociated from the Agarose beads by heating at 95°C for 5 min in Laemmli's sample buffer.

Co-IP experiments on protein extracts from the rolandic area were performed as follows: protein extraction was done as already described (62). Washed brain tissue was homogenized in 4–8 volumes of STMDPS (50 mM Tris, pH 7.4, 250 mM sucrose, 5 mM $MgCl_2$). The homogenate was centrifuged 15 min at 1300g, 4°C and the supernatant was aliquoted and conserved at −80°C. Immunoprecipitations were performed with Size Pimary Immunoprecipitation Kit, according to the manufacturer's protocol (Pierce): after washing with coupling buffer, 100 µl of AminoLink Plus 50% Gel Slurry were incubated overnight with 50 µg of rabbit anti-SRPX2 antibody (Supplementary Material, Fig. S5) (7) or non-immune rabbit IgG (Jackson Laboratories) diluted in 200 µl of coupling buffer + 2 µl of Reducing Agent. After several washes, the antibody-coupled gel was incubated overnight at 4°C with 500 µl of protein extract. Proteins were then eluted in 3 × 50 µl of ImmunoPure Elution buffer.

Western blot analysis

After separation on SDS-containing 7–10% polyacrylamide gels (SDS–PAGE), the proteins were transferred on a nitrocellulose membrane (Protran, Schleicher and Schuell). After blocking the non-specific sites with 5% non-fat milk in Tris buffered saline, the membrane was incubated with primary antibodies: mouse anti-myc (1/5000, Roche), mouse anti-GFP (1/8000, Clontech), mouse anti-GAPDH (1/10 000, Chemicon), rabbit anti-SRPX2 (1/500, PTG-Lab; Supplementary Material, Fig. S5) or rabbit anti-uPAR (1/500, American

Diagnostica) for 1 h to overnight, and then incubated with anti-mouse or anti-rabbit HRP-conjugated antibodies (1/5000, Jackson Immunoresearch). The membrane were revealed with ECL Plus Western Blotting Detection System (Amersham, GE Healthcare) and exposed to autoradiographic film (BioMax MS films, Eastman-Kodak).

Immunocyto- and immunohistochemistry

COS-7 cells were transfected as described earlier and fixed in 4% paraformaldehyde for 20 min at room temperature and then neutralized with 50 mM NH_4Cl. Non-specific binding was blocked in 0.1 M sodium phosphate, pH 7.4, with 10% normal goat serum, supplemented with 0.5% Triton X-100. Cells were incubated with a polyclonal anti-uPAR antibody (1/400, American Diagnostica). The secondary antibodies were anti-rabbit antibodies conjugated to Alexa 488 (1/400, Invitrogen). Coverslips were mounted in Vectashield (Vector). Images were obtained with confocal microscope Leica TCS SP5, 1024 × 1024 pixel images, 0.2 µm step, ×3 line average, ×3 frame accumulation.

Immunohistochemistry experiments were performed as already described (7). Briefly, human and Wistar rat adult brain tissues were frozen with liquid nitrogen vapors and stored at −80°C until use. Wistar rat embryos at E16.5 and newborns (P0) were sacrificed and total bodies (E16.5) or heads (P0) were frozen with liquid nitrogen vapors and stored at −80°C until use. Serial sections (14 µm with a Microm cryostat) of human and rat samples were dipped in 4% paraformaldehyde in PBS (pH 7.4) for 30 min and then rinsed in PBS. Paraformaldehyde was neutralized by 0.1 M Glycine. Non-specific binding was blocked and tissue was permeabilized in 0.1 M phosphate buffer, pH 7.4, supplemented with 10% NGS or NHS and 0.01% Triton. Primary antibodies were incubated 1 h to overnight at 37°C. The following antibodies were used as primary antibodies: rabbit anti-SRPX2 antibody (1/50) (7) (Supplementary Material, Fig. S5), rabbit anti-uPAR antibody (1/25, SantaCruz) and mouse anti-MAP2 antibody (1/50, Sigma). Secondary antibodies were incubated 1 h at 37°C using anti-rabbit Alexa 488-conjugated antibodies (1/400, Invitrogen) or anti-mouse Alexa 568-conjugated antibodies (1/400, Invitrogen). For peroxidase detection, the Vectastain ABC kit and its substrate Peroxidase AEC kit (Vector, Abcyss) were used according to the manufacturer's protocol. In each experiment, negative controls included slides incubated with non-immune rabbit or mouse IgG (Jackson Laboratories). Sections were observed with a microscope (Leica, CTR5000) and camera (Leica DFC300FX).

Production of SRPX2 proteins in *P. pastoris*

EasySelect *Pichia* Expression kit (Invitrogen) was used to produce recombinant SRPX2 proteins in *P. pastoris* according to the manufacturer's protocol. Briefly, pPICZ-SRPX2 plasmids for the production of the wild-type, pathogenic mutant (p.Y72S, p.327S) and chimpanzee (R_{75}) SRPX2 proteins were linearized with *Pme*I restriction enzyme and introduced in X-33 strain by EasyComp transformation (Invitrogen). Clones that were able to metabolize methanol were then selected on the basis of protein production efficiency. For production, one

colony was cultured in 25 ml of BMGY medium 30 h at 29°C. The culture was diluted to 1/40 in BMGY and cultured 16 h at 29°C. After centrifugation (3000g, 5′, room temperature), yeast were resuspended at $OD_{600} = 1$ in BMMY and cultured 8 h (wild-type) or 24 h (pathogenic mutants and chimpanzee) at 29°C. Cultures were then centrifuged (3000g, 5′, room temperature) and pellets were stored at −80°C if necessary. Pellets were resuspended in breaking buffer to $50 < OD_{600} < 100$ and equal volume of acid-washed glass beads was added. The mixture was vortexed for 30 s and then incubated on ice for 30 s; this was repeated seven more times and the mixture was then centrifuged (12 000g, 10′, 4°C). The insoluble proteins were extracted from the pellet in the same way in 8 M urea. Protino Ni-IDA columns (Macherey-Nagel) were used to purify the proteins in denaturing conditions, according to the manufacturer's protocol. Briefly, columns were equilibrated in denaturing buffer (50 mM NaH_2PO_4, pH 8.0, 300 mM NaCl, 8 M urea). The samples were then charged and the resin was washed two times. Elution was done in denaturing buffer + 250 mM imidazole. The first fraction of elution was concentrated about 10-folds on Amicon (Millipore) and dialyzed in Slide-a-lyser cassettes (Pierce) against 10 mM NaH_2PO_4, pH 8.0, 300 mM NaCl, 0,05% Tween20.

Protein production and purification were checked by SDS–PAGE and by mass spectrometry (Supplementary Material, Fig. S4). For mass spectrometry, proteins were 'in gel' digested in excised gel plugs, using sequencing grade modified porcine trypsin (12.5 ng/l, Promega). The peptides were extracted, dried in a vacuum, centrifuged and resuspended in 10–20 μl of 0.1% TFA.

For MALDI mass spectrometry identification (wt and R_{75} SRPX2 proteins), the peptide mixture resulting from protein digestion was then analyzed using a Ettan pro MALDI time-of-flight mass spectrometer (Amersham biosciences) in positive ion reflector mode. 0.3 μl of the Peptide mixture was co-crystallized on the MALDI target with an equal amount of matrix solution (3 mg/ml of α-cyano-4-hydroxycinnamic acid in 50% acetonitrile) in the presence of 0.5% TFA. Alternatively, peptide mixtures derived from proteins were desalted and concentrated using zip tips (Millipore) and deposited onto the MALDI target by elution with the matrix solution. Proteins were identified by the Mascot (Matrix science Ltd) software that queries Swissprot database.

For Nano electrospray MS/MS identification (p.Y72S SRPX2 protein), mass spectrometric measurements were done on a LCQ^{TM} Deca XP Plus ion trap mass spectrometer (ThermoFinnigan) equipped with a LCQ^{TM} nanospray ionization source. Digested peptides were separated using an Ettan MDLC chromatographic system (GE Healthcare). The chromatographic system was piloted by Unicorn 5.01 software (GE Healthcare). Three dependant MS/MS spectra of the three most intense peaks were collected following one full scan mass spectrum. Extracted MS/MS spectra were automatically assigned to the best matching peptide sequence using the Mascot software against Swissprot Database.

SPR analysis of SRPX2/uPAR interactions

SPR experiments were performed at 25°C on a CM5 sensor chip with a Biacore 3000 instrument (GE Healthcare). GST

(control flow cell) or GST-uPAR (experiment flow cell) proteins were covalently immobilized (50–80 fmol) using amine coupling chemistry according to the manufacturer's instructions. GST protein was produced as already described (27) and GST-uPAR fusion protein was obtained from Abnova Ltd. The single-cycle kinetic method (26,27) was used to analyze the binding of SRPX2 proteins (wild-type, pY72S and R_{75}) to GST-uPAR (Supplementary Material, Fig. S6). SRPX2 proteins were serially diluted 2-fold in running buffer (10 mM NaH_2PO_4, 300 mM NaCl, 0.05% Tween20), yielding concentrations ranging from 7 to 115 nM. Samples were injected sequentially at 30 μl/min in increasing concentrations over both the ligand and the reference surfaces. Blank runs (buffer) were also included prior to SRPX2 injections and used to double-reference the binding data. Sensorgrams obtained with control flow cell were systematically subtracted from those obtained with GST-uPAR flow cells. Subtracted sensorgrams were globally fitted with the 1:1 titration kinetic binding model with BIAevaluation 4.1 software. Three independent experiments were done and used to calculate an average K_D for each uPAR-binding of SRPX2 wild-type and mutant proteins (Table 3).

URLs

We used the following websites for genes, proteins, diseases and sequence alignements: Golden path sequence assembly (http://genome.ucsc.edu/), BLAST, OMIM and Genbank at NCBI (http://www.ncbi.nlm.nih.gov/), Human Protein Reference Database (http://www.hprd.org/).

SUPPLEMENTARY MATERIAL

Supplementary Material is available at *HMG* Online.

FUNDING

ACKNOWLEDGEMENTS

REFERENCES

1. Sun, T., Patoine, C., Abu-Khalil, A., Visvader, J., Sum, E., Cherry, T.J., Orkin, S.H., Geschwind, D.H. and Walsh, C.A. (2005) Early asymmetry of gene transcription in embryonic human left and right cerebral cortex. *Science*, **308**, 1794–1798.

2. Abrahams, B.S., Tentler, D., Perederiy, J.V., Oldham, M.C., Coppola, G. and Geschwind, D.H. (2007) Genome-wide analyses of human perisylvian cerebral cortical patterning. *Proc. Natl. Acad. Sci. USA*, **104**, 17849–17854.

3. Lai, C.S., Fisher, S.E., Hurst, J.A., Vargha-Khadem, F. and Monaco, A.P. (2001) A forkhead-domain gene is mutated in a severe speech and language disorder. *Nature*, **413**, 519–523.

4. White, S.A., Fisher, S.E., Geschwind, D.H., Scharff, C. and Holy, T.E. (2006) Singing mice, songbirds, and more: models for FOXP2 function and dysfunction in human speech and language. *J. Neurosci.*, **26**, 10376–10379.

5. Spiteri, E., Konopka, G., Coppola, G., Bomar, J., Oldham, M., Ou, J., Vernes, S.C., Fisher, S.E., Ren, B. and Geschwind, D.H. (2007) Identification of the transcriptional targets of FOXP2, a gene linked to speech and language, in developing human brain. *Am. J. Hum. Genet.*, **81**, 1144–1157.

6. Vernes, S.C., Spiteri, E., Nicod, J., Groszer, M., Taylor, J.M., Davies, K.E., Geschwind, D.H. and Fisher, S.E. (2007) High-throughput analysis of promoter occupancy reveals direct neural targets of FOXP2, a gene mutated in speech and language disorders. *Am. J. Hum. Genet.*, **81**, 1232–1250.

7. Roll, P., Rudolf, G., Pereira, S., Royer, B., Scheffer, I.E., Massacrier, A., Valenti, M.P., Roeckel-Trevisiol, N., Jamali, S., Beclin, C. *et al.* (2006) SRPX2 mutations in disorders of language cortex and cognition. *Hum. Mol. Genet.*, **15**, 1195–1207.

8. O'Leary, J.M., Bromek, K., Black, G.M., Uhrinova, S., Schmitz, C., Wang, X., Krych, M., Atkinson, J.P., Uhrin, D. and Barlow, P.N. (2004) Backbone dynamics of complement control protein (CCP) modules reveals mobility in binding surfaces. *Protein Sci.*, **13**, 1238–1250.

9. Jacobson, L.H., Kelly, P.H., Bettler, B., Kaupmann, K. and Cryan, J.F. (2006) GABA(B(1)) receptor isoforms differentially mediate the acquisition and extinction of aversive taste memories. *J. Neurosci.*, **26**, 8800–8803.

10. Vigot, R., Barbieri, S., Bräuner-Osborne, H., Turecek, R., Shigemoto, R., Zhang, Y.P., Luján, R., Jacobson, L.H., Biermann, B., Fritschy, J.M. *et al.* (2006) Differential compartmentalization and distinct functions of GABAB receptor variants. *Neuron*, **50**, 589–601.

11. Gunnersen, J.M., Kim, M.H., Fuller, S.J., De Silva, M., Britto, J.M., Hammond, V.E., Davies, P.J., Petrou, S., Faber, E.S., Sah, P. and Tan, S.S. (2007) Sez-6 proteins affect dendritic arborization patterns and excitability of cortical pyramidal neurons. *Neuron*, **56**, 621–639.

12. Hoshino, M., Matsuzaki, F., Nabeshima, Y. and Hama, C. (1993) Hikaru genki, a CNS-specific gene identified by abnormal locomotion in *Drosophila*, encodes a novel type of protein. *Neuron*, **10**, 395–407.

13. Kurosawa, H., Goi, K., Inukai, T., Inaba, T., Chang, K.S., Shinjyo, T., Rakestraw, K.M., Naeve, C.W. and Look, A.T. (1999) Two candidate downstream target genes for E2A-HLF. *Blood*, **93**, 321–332.

14. Oleszewski, M., Gutwein, P., von der Lieth, W., Rauch, U. and Altevogt, P. (2000) Characterization of the L1-neurocan-binding site implications for L1-L1 homophilic binding. *J. Biol. Chem.*, **275**, 34478–34485.

15. Jenkins, H.T., Mark, L., Ball, G., Persson, J., Lindahl, G., Uhrin, D., Blom, A.M. and Barlow, P.N. (2006) Human C4b-binding protein - structural basis for interaction with streptococcal M protein, a major bacterial virulence factor. *J. Biol. Chem.*, **281**, 3690–3697.

16. Wei, Xq., Orchardson, M., Gracie, J.A., Leung, B.P., Gao, Bm., Guan, H., Niedbala, W., Paterson, G.K., McInnes, I.B. and Liew , F.Y. (2001) The Sushi domain of soluble IL-15 receptor alpha is essential for binding IL-15 and inhibiting inflammatory and allogenic responses *in vitro* and *in vivo*. *J. Immunol.*, **167**, 277–282.

17. Hanick, N.A., Rickert, M., Varani, L., Bankovich, A.J., Cochran, J.R., Kim, D.M., Surh, C.D. and Garcia, K.C. (2007) Elucidation of the interleukin-15 binding site on its alpha receptor by NMR. *Biochemistry*, **46**, 9453–9461.

18. Sirerol-Piquer, M.S., Ayerdi-Izquierdo, A., Morante-Redolat, J.M., Herranz-Pérez, V., Favell, K., Barker, P.A. and Pérez-Tur, J. (2006) The epilepsy gene LGI1 encodes a secreted glycoprotein that binds to the cell surface. *Hum. Mol. Genet.*, **15**, 3436–3445.

19. Fukata, Y., Adesnik, H., Iwanaga, T., Bredt, D.S., Nicoll, R.A. and Fukata, M. (2006) Epilepsy-related ligand/receptor complex LGI1 and ADAM22 regulate synaptic transmission. *Science*, **313**, 1792–1795.

20. Schulte, U., Thumfart, J.O., Klöcker, N., Sailer, C.A., Bildl, W., Biniossek, M., Dehn, D., Deller, T., Eble, S., Abbass, K. *et al.* (2006) The epilepsy-linked Lgi1 protein assembles into presynaptic Kv1 channels and inhibits inactivation by Kvbeta1. *Neuron*, **49**, 697–706.

21. Ragno, P. (2006) The urokinase receptor: a ligand or a receptor? Story of a sociable molecule. *Cell Mol. Life Sci.*, **63**, 1028–1037.

22. Powell, E.M., Campbell, D.B., Stanwood, G.D., Davis, C., Noebels, J.L. and Levitt, P. (2003) Genetic disruption of cortical interneuron development causes region- and GABA cell type-specific deficits, epilepsy, and behavioral dysfunction. *J. Neurosci.*, **23**, 622–631.

23. Eagleson, K.L., Bonnin, A. and Levitt, P. (2005) Region- and age-specific deficits in gamma-aminobutyric acidergic neuron development in the telencephalon of the uPAR(−/−) mouse. *J. Comp. Neurol.*, **489**, 449–466.

24. Jo, M., Thomas, K.S., O'Donnell, D.M. and Gonias, S.L. (2003) Epidermal growth factor receptor-dependent and -independent cell-signaling pathways originating from the urokinase receptor. *J. Biol. Chem.*, **278**, 1642–1646.

25. Royer, B., Soares, D.C., Barlow, P.N., Bontrop, R.E., Roll, P., Robaglia-Schlupp, A., Blancher, A., Levasseur, A., Cau, P., Pontarotti, P. and Szepetowski, P. (2007) Molecular evolution of the human SRPX2 gene that causes brain disorders of the Rolandic and Sylvian speech areas. *BMC Genet.*, **8**, 72.

26. Karlsson, R., Katsamba, P.S., Nordin, H., Pol, E. and Myszka, D.G. (2006) Analyzing a kinetic titration series using affinity biosensors. *Anal. Biochem.*, **349**, 136–147.

27. Marquèze-Pouey, B., Martin-Moutot, N., Sakkou-Norton, M., Lévêque, C., Ji, Y., Cornet, V., Hsiao, W.L. and Seagar, M. (2008) Toxicity and endocytosis of spinocerebellar ataxia type 6 polyglutamine domains: role of myosin IIB. *Traffic*, **9**, 1088–1100.

28. Mahdi, F., Shariat-Madar, Z., Kuo, A., Carinato, M., Cines, D.B. and Schmaier, A.H. (2004) Mapping the interaction between high molecular mass kininogen and the urokinase plasminogen activator receptor. *J. Biol. Chem.*, **279**, 16621–16628.

29. Huai, Q., Mazar , A.P., Kuo, A., Parry, G.C., Shaw, D.E., Callahan, J., Li, Y., Yuan, C., Bian, C., Chen, L. *et al.* (2006) Structure of human urokinase plasminogen activator in complex with its receptor. *Science*, **311**, 656–659.

30. Huai, Q., Zhou, A., Lin, L., Mazar, A.P., Parry, G.C., Callahan, J., Shaw, D.E., Furie, B., Furie, B.C. and Huang, M. (2008) Crystal structures of two human vitronectin, urokinase and urokinase receptor complexes. *Nat. Struct. Mol. Biol.*, **15**, 422–423.

31. Ploug, M. and Ellis, V. (1994) Structure-function relationships in the receptor for urokinase-type plasminogen activator. Comparison to other members of the Ly-6 family and snake venom alpha-neurotoxins. *FEBS Lett.*, **349**, 163–168.

32. Dibbens, L.M., Tarpey, P.S., Hynes, K., Bayly, M.A., Scheffer, I.E., Smith, R., Bomar, J., Sutton, E., Vandeleur, L., Shoubridge, C. *et al.* (2008) X-linked protocadherin 19 mutations cause female-limited epilepsy and cognitive impairment. *Nat. Genet.*, **40**, 776–781.

33. Morishita, H. and Yagi, T. (2007) Protocadherin family: diversity, structure, and function. *Curr. Opin. Cell Biol.*, **19**, 584–592.

34. Mondino, A. and Blasi, F. (2004) uPA and uPAR in fibrinolysis, immunity and pathology. *Trends Immunol.*, **25**, 450–455.

35. Alfano, D., Franco, P., Vocca, I., Gambi, N., Pisa, V., Mancini, A., Caputi, M., Carriero, M.V., Iaccarino, I. and Stoppelli, M.P. (2005) The

urokinase plasminogen activator and its receptor: role in cell growth and apoptosis. *Thromb. Haemost.*, **93**, 205–211.

36. Levitt, P. (2005) Disruption of interneuron development. *Epilepsia*, **46** (Suppl. 7), 22–28.

37. Kriegstein, A.R. (2005) Constructing circuits: neurogenesis and migration in the developing neocortex. *Epilepsia*, **46** (Suppl. 7), 15–21.

38. Represa, A. and Ben-Ari, Y. (2005) Trophic actions of GABA on neuronal development. *Trends Neurosci.*, **28**, 278–283.

39. Richards, A., Kemp, E.J., Liszewski, M.K., Goodship, J.A., Lampe, A.K., Decorte, R., Muslumanoglu, M.H., Kavukcu, S., Filler, G., Pirson, Y. *et al.* (2003) Mutations in human complement regulator, membrane cofactor protein (CD46), predispose to development of familial hemolytic uremic syndrome. *Proc. Natl. Acad. Sci. USA*, **100**, 12966–12971.

40. Herbert, A.P., Uhrin, D., Lyon, M., Pangburn, M.K. and Barlow, P.N. (2006) Disease-associated sequence variations congregate in a polyanion-recognition patch on human factor H revealed in 3D structure. *J. Biol. Chem.*, **281**, 16512–16520.

41. Herbert, A., Soares, D.C., Pangburn, M.K. and Barlow, P.N. (2006) Disease-associated sequence variants in factor H: a structural biology approach. *Adv. Exp. Med. Biol.*, **586**, 313–327.

42. Engelholm, L.H. and Behrendt, N. (2001) Differential binding of urokinase and peptide antagonists to the urokinase receptor: evidence from characterization of the receptor in four primate species. *Biol. Chem.*, **382**, 435–442.

43. Mannaioni, G., Orr, A.G., Hamill, C.E., Yuan, H., Pedone, K.H., McCoy, K.L., Palmini, R.B., Junge, C.E., Lee, C.J., Yepes, M. *et al.* (2008) Plasmin potentiates synaptic *N*-methyl-D-aspartate receptor function in hippocampal neurons through activation of protease-activated receptor-1. *J. Biol. Chem.*, **283**, 20600–20611.

44. Tsirka, S.E., Gualandris, A., Amaral, D.G. and Strickland, S. (1995) Excitotoxin-induced neuronal degeneration and seizure are mediated by tissue plasminogen activator. *Nature*, **377**, 340–344.

45. Lahtinen, L., Lukasiuk, K. and Pitkänen, A. (2006) Increased expression and activity of urokinase-type plasminogen activator during epileptogenesis. *Eur. J. Neurosci.*, **24**, 1935–1945.

46. Meiri, N., Masos, T., Rosenblum, K., Miskin, R. and Dudai, Y. (1994) Overexpression of urokinase-type plasminogen activator in transgenic mice is correlated with impaired learning. *Proc. Natl. Acad. Sci. USA*, **91**, 3196–3200.

47. Powell, E.M., Mars, W.M. and Levitt, P. (2001) Hepatocyte growth factor/scatter factor is a motogen for interneurons migrating from the ventral to dorsal telencephalon. *Neuron*, **30**, 79–89.

48. Molinari, F., Rio, M., Meskenaite, V., Encha-Razavi, F., Augé, J., Bacq, D., Briault, S., Vekemans, M., Munnich, A., Attié-Bitach, T. *et al.* (2002) Truncating neurotrypsin mutation in autosomal recessive nonsyndromic mental retardation. *Science*, **298**, 1779–1781.

49. Lehesjoki, A.-E. (2003) Molecular background of progressive myoclonus epilepsy. *EMBO J.*, **22**, 3473–3478.

50. Mueller-Steiner, S., Zhou, Y., Arai, H., Roberson, E.D., Sun, B., Chen, J., Wang, X., Yu, G., Esposito, L., Mucke, L. and Gan, L. (2006) Antiamyloidogenic and neuroprotective functions of cathepsin B: implications for Alzheimer's disease. *Neuron*, **51**, 703–714.

51. Hamel, M.G., Ajmo, J.M., Leonardo, C.C., Zuo, F., Sandy, J.D. and Gottschall, P.E. (2008) Multimodal signaling by the ADAMTSs (a disintegrin and metalloproteinase with thrombospondin motifs) promotes neurite extension. *Exp. Neurol.*, **210**, 428–440.

52. Galtrey, C.M. and Fawcett, J.W. (2007) The role of chondroitin sulfate proteoglycans in regeneration and plasticity in the central nervous system. *Brain Res. Rev.*, **54**, 1–18.

53. Steinlein, O.K. (2004) Genetic mechanisms that underlie epilepsy. *Nat. Rev. Neurosci.*, **5**, 400–408.

54. Berkovic, S.F., Mulley, J.C., Scheffer, I.E. and Petrou, S. (2006) Human epilepsies: interaction of genetic and acquired factors. *Trends Neurosci.*, **29**, 391–397.

55. Jansen, A. and Andermann, E. (2005) Genetics of the polymicrogyria syndromes. *J. Med. Genet.*, **42**, 369–378.

56. Guerrini, R., Dobyns, W.B. and Barkovich, A.J. (2008) Abnormal development of the human cerebral cortex: genetics, functional consequences and treatment options. *Trends Neurosci.*, **31**, 154–162.

57. Vojtek, A.B. and Hollenberg, S.M. (1995) Ras-Raf interaction: two-hybrid analysis. *Methods Enzymol.*, **255**, 331–342.

58. Bartel, P., Chien, C.T., Sternglanz, R. and Fields, S. (1993) Elimination of false positives that arise in using the two-hybrid system. *Biotechniques*, **14**, 920–924.

59. Fromont-Racine, M., Rain, J.C. and Legrain, P. (1997) Toward a functional analysis of the yeast genome through exhaustive two-hybrid screens. *Nat. Genet.*, **16**, 277–282.

60. Formstecher, E., Aresta, S., Collura, V., Hamburger, A., Meil, A., Trehin, A., Reverdy, C., Betin, V., Maire, S., Brun, C. *et al.* (2005) Protein interaction mapping: a *Drosophila* case study. *Genome Res.*, **15**, 376–384.

61. Flanagan, J.G., Cheng, H.J., Feldheim, D.A., Hattori, M., Lu, Q. and Vanderhaeghen, P. (2000) Alkaline phosphatase fusions of ligands or receptors as in situ probes for staining of cells, tissues, and embryos. *Methods Enzymol.*, **327**, 19–35.

62. Cox, B. and Emili, A. (2006) Tissue subcellular fractionation and protein extraction for use in mass-spectrometry-based proteomics. *Nat. Protoc.*, **1**, 1872–1878.

63. Yamaji, R., Chatani, E., Harada, N., Sugimoto, K., Inui, H. and Nakano, Y. (2005) Glyceraldehyde-3-phosphate dehydrogenase in the extracellular space inhibits cell spreading. *Biochim. Biophys. Acta*, **1726**, 261–271.

64. Houseweart, M.K., Pennacchio, L.A., Vilaythong, A., Peters, C., Noebels, J.L. and Myers, R.M. (2003) Cathepsin B but not cathepsins L or S contributes to the pathogenesis of Unverricht-Lundborg progressive myoclonus epilepsy (EPM1). *J. Neurobiol.*, **56**, 315–327.

65. Nakamura, H., Fujii, Y., Inoki, I., Sugimoto, K., Tanzawa, K., Matsuki, H., Miura, R., Yamaguchi, Y. and Okada, Y. (2000) Brevican is degraded by matrix metalloproteinases and aggrecanase-1 (ADAMTS4) at different sites. *J. Biol. Chem.*, **275**, 38885–38890.

66. Westling, J., Gottschall, P.E., Thompson, V.P., Cockburn, A., Perides, G., Zimmermann, D.R. and Sandy, J.D. (2004) ADAMTS4 (aggrecanase-1) cleaves human brain versican V2 at Glu405-Gln406 to generate glial hyaluronate binding protein. *Biochem. J.*, **377**, 787–795.

67. Suzuki, S.T. (2000) Recent progress in protocadherin research. *Exp. Cell Res.*, **261**, 13–18.

68. Uemura, M., Nakao, S., Suzuki, S.T., Takeichi, M. and Hirano, S. (2007) OL-Protocadherin is essential for growth of striatal axons and thalamocortical projections. *Nat. Neurosci.*, **10**, 1151–1159.

69. Aihara, K., Kuroda, S., Kanayama, N., Matsuyama, S., Tanizawa, K. and Horie, M. (2003) A neuron-specific EGF family protein, NELL2, promotes survival of neurons through mitogen-activated protein kinases. *Brain Res. Mol. Brain Res.*, **116**, 86–93.

70. Matsuyama, S., Doe, N., Kurihara, N., Tanizawa, K., Kuroda, S., Iso, H. and Horie, M. (2005) Spatial learning of mice lacking a neuron-specific epidermal growth factor family protein, NELL2. *J. Pharmacol. Sci.*, **98**, 239–243.

71. Zhou, C.J., Borello, U., Rubenstein, J.L. and Pleasure, S.J. (2006) Neuronal production and precursor proliferation defects in the neocortex of mice with loss of function in the canonical Wnt signaling pathway. *Neuroscience*, **142**, 1119–1131.